Author/s:
Oliver, KL;Franceschetti, S;Milligan, CJ;Muona, M;Mandelstam, SA;Canafoglia, L;Boguszewska-Chachulska, AM;Korczyn, AD;Bisulli, F;Di Bonaventura, C;Ragona, F;Michelucci, R;Ben-Zeev, B;Straussberg, R;Panzica, F;Massano, J;Friedman, D;Crespel, A;Engelsen, BA;Andermann, F;Andermann, E;Spodar, K;Lasek-Bal, A;Riguzzi, P;Pasini, E;Tinuper, P;Licchetta, L;Gardella, E;Lindenau, M;Wulf, A;Møller, RS;Benninger, F;Afawi, Z;Rubboli, G;Reid, CA;Maljevic, S;Lerche, H;Lehesjoki, AE;Petrou, S;Berkovic, SF

Title:
Myoclonus epilepsy and ataxia due to KCNC1 mutation: Analysis of 20 cases and K+ channel properties

Date:
2017-05-01

Citation:
Oliver, K. L., Franceschetti, S., Milligan, C. J., Muona, M., Mandelstam, S. A., Canafoglia, L., Boguszewska-Chachulska, A. M., Korczyn, A. D., Bisulli, F., Di Bonaventura, C., Ragona, F., Michelucci, R., Ben-Zeev, B., Straussberg, R., Panzica, F., Massano, J., Friedman, D., Crespel, A., Engelsen, B. A. ,... Berkovic, S. F. (2017). Myoclonus epilepsy and ataxia due to KCNC1 mutation: Analysis of 20 cases and K+ channel properties. Annals of Neurology, 81 (5), pp.677-689. https://doi.org/10.1002/ana.24929.

	Lindenau, Matthias; Epilepsy Center Hamburg-Alsterdorf Wulf, Annette; Epilepsy Center Hamburg-Alsterdorf Møller, Rikke; Danish Epilepsy Centre, Benninger, Felix; Rabin Medical Center, Neurology Afawi, Zaid; Tel Aviv University Sackler Faculty of Medicine Rubboli, Guido; University of Copenhagen, Reid, Christopher; The Florey Institute of Neuroscience and Mental Health, Ion Channels and Disease Maljevic, Snezana; The Florey Institute of Neuroscience and Mental Health, Ion Channels and Disease Lerche, Holger; University of Tuebingen, Neurology and Epileptology Lehesjoki, Anna-Elina; University of Helsinki, Neuroscience Center Petrou, Steven; The Florey Institute of Neuroscience and Mental Health, Ion Channels and Disease Berkovic, Samuel; Epilepsy Research Centre,

Keywords:	Ataxia, Progressive Myoclonus Epilepsy, Potassium ion channels
Domain:	Immunology and/or Genetics

Note: The following files were submitted by the author for peer review, but cannot be converted to PDF. You must view these files (e.g. movies) online.

MEAK_video.mp4

Myoclonus epilepsy and ataxia due to *KCNC1* mutation:

Analysis of 20 cases and K^+ channel properties

Karen L Oliver MSc,[1] Silvana Franceschetti MD, PhD,[2] Carol J Milligan PhD,[3] Mikko Muona PhD,[4-7] Simone A Mandelstam MBChB,[8-10] Laura Canafoglia MD, PhD,[2] Anna M Boguszewska-Chachulska PhD,[11] Amos Korczyn MD,[12] Francesca Bisulli MD, PhD,[13,14] Carlo Di Bonaventura MD, PhD,[15] Francesca Ragona MD,[16] Roberto Michelucci MD, PhD,[13,17] Bruria Ben-Zeev MD,[12,18] Rachel Straussberg MD,[12,19] Ferruccio Panzica MSc,[2] João Massano MD,[20,21] Daniel Friedman MD, MS,[22] Arielle Crespel MD,[23] Bernt A Engelsen MD, PhD,[24] Frederick Andermann MD,[25,26] Eva Andermann MD, PhD,[27,28] Krystyna Spodar MD, PhD,[11] Anetta Lasek-Bal MD, PhD,[29] Patrizia Riguzzi MD,[13,17] Elena Pasini MD,[13,17] Paolo Tinuper MD,[13,14] Laura Licchetta MD,[13,14] Elena Gardella MD, PhD,[30,31] Matthias Lindenau MD,[32] Annette Wulf MD,[32] Rikke S Møller PhD,[30,31] Felix Benninger MD,[33] Zaid Afawi MD, PhD,[12] Guido Rubboli MD,[13,34] Christopher A Reid PhD,[3] Snezana Maljevic PhD,[3,35] Holger Lerche MD,[35] Anna-Elina Lehesjoki MD, PhD,[5-7] Steven Petrou PhD,[3,36] Samuel F Berkovic MD, FRS[1]

1. Epilepsy Research Centre, Department of Medicine, The University of Melbourne, Austin Health, Heidelberg, Victoria, Australia
2. Department of Neurophysiology, C. Besta Neurological Institute IRCCS Foundation, Milan, Italy
3. Ion Channels & Disease Group, Epilepsy Division, The Florey Institute of Neuroscience and Mental Health, Parkville, Victoria, Australia
4. Institute for Molecular Medicine Finland, University of Helsinki, Helsinki, Finland
5. Folkhälsan Institute of Genetics, Helsinki, Finland
6. Research Programs Unit, Molecular Neurology, University of Helsinki, Helsinki, Finland
7. Neuroscience Center, University of Helsinki, Helsinki, Finland
8. The Florey Institute of Neuroscience and Mental Health, Melbourne, Australia
9. Departments of Paediatrics and Radiology, The University of Melbourne, Melbourne, Australia
10. Department of Medical Imaging, Royal Children's Hospital, Melbourne, Australia

11. Genomed Health Care Center, Genomed SA, Warsaw, Poland
12. Sackler Faculty of Medicine, Tel Aviv University, Tel Aviv, Israel
13. IRCCS-Institute of Neurological Sciences of Bologna, Bologna, Italy
14. Department of Biomedical and Neuromotor Sciences, University of Bologna, Bologna, Italy
15. Department of Neurological Sciences, University of Rome, La Sapienza, Rome, Italy
16. Department of Pediatric Neuroscience, C. Besta Neurological Institute IRCCS Foundation, Milan, Italy
17. Unit of Neurology, Bellaria Hospital, Bologna, Italy
18. The Edmond and Lily Safra Children's Hospital, Sheba Medical Center, Ramat Gan, Israel
19. Epilepsy Unit, Schneider Children's Medical Center of Israel, Petah Tikvah, Israel
20. Department of Neurology, Hospital Pedro Hispano/ULS Matosinhos, Portugal
21. Department of Clinical Neurosciences and Mental Health, Faculty of Medicine University of Porto, Portugal
22. Comprehensive Epilepsy Center, New York University Langone Medical Center, New York, NY, USA
23. Epilepsy Unit, Hôpital Gui de Chauliac, Montpellier, France
24. Department of Clinical Medicine, University of Bergen, Norway
25. Epilepsy Research Group, Montreal Neurological Hospital and Institute, Montreal, Quebec, Canada
26. Departments of Neurology & Neurosurgery and Peadiatrics, McGill University, Montreal, Quebec, Canada
27. Neurogenetics Unit and Epilepsy Research Group, Montreal Neurological Hospital and Institute, Montreal, Quebec, Canada
28. Departments of Neurology & Neurosurgery and Human Genetics, McGill University, Montreal, Quebec, Canada
29. High School of Science, Medical University of Silesia, Department of Neurology, Upper Silesian Medical Centre, Katowice, Poland
30. Danish Epilepsy Centre, Dianalund, Denmark
31. Institute for Regional Health research, University of Southern Denmark, Odense, Denmark

32. Department of Neurology and Epileptology, Epilepsy Center Hamburg-Alsterdorf, Hamburg, Germany
33. Department of Neurology, Rabin Medical Center, Beilinson Hospital, Petah Tikvah, Israel
34. Danish Epilepsy Centre, Filadelfia/University of Copenhagen, Dianalund, Denmark
35. University of Tübingen, Department of Neurology and Epileptology, Hertie Institute for Clinical Brain Research, Germany
36. Centre for Neural Engineering, Department of Electrical Engineering, University of Melbourne, Parkville, Victoria, Australia

Corresponding author:

Prof Samuel Berkovic

Address: 245 Burgundy St. Heidelberg, VIC. Australia 3084

Phone: +61 3 9035 7093 | Fax: +61 3 9496 2291 | Email: s.berkovic@unimelb.edu.au

Running head: Myoclonus, epilepsy, ataxia due to *KCNC1*

Number of characters in Title: 99
Number of characters in Running head: 40
Number of words in Abstract: 250
Number of words in Main text: 4602
Number of Figures: 7
Number of Tables: 1
Number of References: 47

Abstract

Objective:

To comprehensively describe the new syndrome of myoclonus epilepsy and ataxia due to potassium (K^+) channel mutation (MEAK), including cellular electrophysiological characterization of observed clinical improvement with fever.

Methods:

We analysed clinical, electroclinical and neuroimaging data for twenty patients with MEAK due to recurrent *KCNC1* p.R320H mutation. *In vitro* electrophysiological studies were conducted using whole cell patch clamp to explore biophysical properties of wild-type and mutant $K_V3.1$ channels.

Results:

Symptoms began between 3-15 years (median 9.5) with progressively severe myoclonus and rare tonic-clonic seizures. Ataxia was present early but quickly became overshadowed by myoclonus; ten patients were wheelchair-bound by late teenage. Mild cognitive decline occurred in half. Early death was not observed. EEG showed generalized spike and polyspike wave discharges with documented photosensitivity in most. Polygraphic EEG-EMG studies demonstrated a cortical origin for myoclonus and striking co-activation of agonist and antagonist muscles. MRI revealed symmetrical cerebellar atrophy, that appeared progressive, and a prominent corpus callosum. Unexpectedly, transient clinical improvement with fever was noted in six patients. To explore this, we performed high temperature *in vitro* recordings. At elevated temperatures there was a robust left-shift in activation of wild-type $K_V3.1$ increasing channel availability.

Interpretation:

MEAK has a relatively homogeneous presentation resembling Unverricht-Lundborg disease, despite the genetic and biological basis being quite different. A remarkable improvement with fever may be explained by the temperature-dependent left-shift in activation of wild-type $K_V3.1$ subunit containing channels that would counter the loss-of-function observed for mutant channels, highlighting *KCNC1* as a potential target for precision therapeutics.

Introduction

Progressive myoclonus epilepsy (PME) is a distinctive epilepsy syndrome characterised by myoclonus, generalised tonic-clonic seizures and progressive neurological deterioration. PME is caused by a number of genetic abnormalities, the majority of which are autosomal recessive conditions. The more frequent disorders are Unverricht-Lundborg disease (ULD), Lafora disease and the neuronal ceroid lipofuscinoses (NCLs) [1, 2]. Rarer recessive disorders include Gaucher disease, action myoclonus renal failure syndrome (AMRF), North Sea PME and sialidoses [3-6]. Mitochondrial inheritance is seen with MERRF [7], whereas, dominantly inherited PMEs include DRPLA [8], juvenile Huntington disease [9], neuroserpinopathy [10] and one form of Kufs disease [11].

Some of the disorders have a geographical concentration such as ULD in Finland and around the Mediterranean, action myoclonus renal failure syndrome in Quebec, DRPLA in Japan and North Sea PME in the Netherlands, Denmark and northern Germany. In carefully studied cohorts, a specific diagnosis can be reached in 70-90% of PME patients [2, 12, 13].

To address the residuum that defied molecular diagnosis we formed an international consortium to collect, characterize and perform whole exome sequencing (WES) on a cohort of 84 hitherto unsolved PME patients. Interrogation of WES data resulted in the discovery of a mutation in the potassium channel gene *KCNC1* [14], a gene not previously associated with human disease, that encodes the voltage-dependent K^+ channel $K_V3.1$. Remarkably, the exact same heterozygous missense change (p.R320H) was found in multiple unrelated patients, the majority of which were sporadic cases due to *de novo* mutation. The mutation was shown to have a dominant-negative loss-of-function effect when the $K_V3.1$ channel was analysed *in vitro* [14].

Here we describe in detail the clinical, electrophysiological and imaging features of this novel disorder known as myoclonus epilepsy and ataxia due to potassium (K^+) channel mutation (MEAK) [14] in twenty patients. Further, we performed additional *in vitro* electrophysiological studies aimed at exploring the clinical observation of improvement with fever.

Materials and Methods

Patients

Twenty patients with the *KCNC1* (c.959G>A; p.R320H; NM_001112741) mutation were identified. These comprised 16 patients previously briefly described [14]; twelve were unrelated sporadic cases and four were from one family. Four additional patients have since been discovered. Two sporadic cases were found via clinical WES and gene panel testing. In a mother-son pair, the diagnosis was suspected clinically and confirmed by Sanger sequencing. Segregation of the variant was determined by Sanger sequencing in each pedigree where DNA from additional family members was available.

We systematically collated clinical data on birth and development, age of disease onset, seizure types, motor symptoms, cognition, medications taken, disease progression and outcome. Electrophysiological and neuroimaging data were collected and analysed as a single cohort. As the cases had been ascertained over many years, the quality and completeness of the data varied.

To demonstrate the cortical origin of reflex/movement activated myoclonus, EEG-EMG signals were analysed using autoregressive parametric modelling, and coherence and phase spectra were evaluated to identify the cortico-muscular relationship [15]. Somatosensory evoked potentials and C reflexes were estimated using standard procedures [16].

The Ethics Committee at the Austin Hospital (Melbourne, Australia) approved this study. Written informed consent was obtained from all patients following local Institutional Review Board requirements.

Cell culture and transfection

The mutation c.959G>A (p.R320H) was inserted in the human *KCNC1* cDNA (NM_004976) cloned in a pCMV-Entry vector (OriGene Technologies) using Quick Change kit (Stratagene) as previously described [14]. Cells were maintained in Modified Eagle's Medium (Sigma, USA) supplemented with 10% (v/v) fetal bovine serum

(Invitrogen), 2 mM L-glutamine (Sigma, USA), 100 U ml^{-1} penicillin and 100 mg ml^{-1} streptomycin (Invitrogen) and 400 µg/ml geneticin (Invitrogen) for up to 30 passages. Cells were kept in humidified 95 % air/5 % CO_2 environment at 37 °C (Thermo scientific, Australia). The cells were grown in T25 cm^2 flasks (BD Biosciences, San Jose, CA, USA) to ~70 % confluency, and then transfected with 9 µg of the human $K_V3.1^{R320H}$ plasmid using Lipofectamine-LTX™ (Invitrogen) in a HEK 293 cell line stably expressing $K_V3.1$.

In vitro electrophysiology

Forty-eight hours post-transfection, the cells were detached using 0.5 mL Accutase® Cell Detachment Solution (Innovative Cell Technologies Inc., San Diego, CA, USA) and resuspended at a density of $1x10^6$ to $5x10^7$ per mL in 50 % MEM (without FBS) and 50 % external recording solution v/v. The external recording solution comprised (mmol/L): 140 NaCl, 4 KCl, 1 $MgCl_2$, 2 $CaCl_2$, 5 D-glucose, 10 HEPES (pH 7.4 with NaOH; ~298 mOsm). The internal recording solution comprised (mmol/L): 50 KCl, 10 NaCl, 60 KF, 20 EGTA, 10 HEPES (pH 7.2 with KOH; ~285 mOsm). Solutions were filtered using a 0.2 µm membrane filter (Minisart; Sartorius Stedim Biotech, Goettingen, Germany). Cells were kept in suspension by gentle automatic pipetting.

Potassium currents generated by $K_v3.1$ channels were recorded using the Patchliner® (Nanion Technologies, Munich, Germany) in the whole-cell configuration. Medium single-hole planar NPC-16 chips with an average resistance of ~2.5 MΩ were used. Pipette and whole cell capacitance were fully compensated. Recordings were acquired at 2 kHz with the low pass filter set to 1 kHz in PATCHMASTER (HEKA Instruments Inc., NY, USA) and performed at 27 °C, 36 °C or 39 °C. To record expressed membrane currents, the cells were held at -80 mV, and 2 s duration test depolarisations were applied in 10 mV increments, from -80 mV to +80 mV, every 7 s. Peak current amplitudes were measured at the beginning of each 2 s depolarizing pulse (mean 0.005 - 0.015 ms). At each temperature, the peak current amplitude at +80 mV for $K_V3.1^{WT+R320H}$ was normalized to the peak current amplitude at +80 mV for $K_V3.1^{WT}$.

Conductance was determined using $G = I / (V-V_r)$, where G is conductance, V is test potential; and V_r is reversal potential. The reversal potential at each temperature was

estimated according to the Nernst equation. The conductance values were then fit with the Boltzmann equation $G = 1 / (1 + \exp[(V-V_{0.5}) / k])$, where V is the potential of the given pulse, $V_{0.5}$ is the potential for the half-maximal activation and k is the slope factor.

Offline analysis was performed using Microsoft Excel and GraphPad Prism 6 (Graphpad Software, La Jolla, USA). Data are shown as means ± S.E.M. Leak subtraction was performed in software before the currents were normalised. Statistical analysis was performed using Student's *t*-test and differences were considered significant when $p<0.05$. Bonferroni correction was applied to take into account multiple comparisons.

Results

The 20 patients comprised 10 females and males, from 16 unrelated families. The patients were aged 17–63 years at the time of the study (Supplementary Table).

Genetic Architecture

Twelve of the sixteen unrelated probands were from Europe. They were not confined to a particular geographic area and included cases extending from Scandinavia to Italy, and from Portugal to Moldova. Two probands were from North America; one of Italian and one of French origin. Two were Israeli of Sephardic Jewish ancestry, originating from Turkey and Tunisia respectively.

Six cases were familial, from two unrelated families. The previously reported Sephardic Jewish family comprised four affected individuals in two generations [14]. The new Italian family comprised a mother-son pair. The parents of the affected mother were unaffected and she had an unaffected brother, suggesting the mutation likely arose *de novo* in her. Maternal DNA was available for the affected mother and tested negative for the *KCNC1* (c.959G>A; p.R320H) mutation. Paternal DNA was not available.

The fourteen remaining cases were sporadic and the mutation was shown to be *de novo* in ten where DNA was available from both parents. In these ten cases the maternal (26.0 ± 5.2 years) and paternal (28.5 ± 5.7 years) ages at conception were known.

Antecedents

No significant antecedent factors for epilepsy were identified and the majority of patients were developmentally normal prior to disease onset (Supplementary Table). The exceptions included familial Cases 12-14 where there were mild motor and learning difficulties. It was possible that this was at least partly due to the married-in father who had learning difficulties. Unrelated Cases 5, 19 and 20 also had mild learning difficulties noted in school, prior to disease onset.

Disease onset

Onset of the progressive neurological syndrome was between 3-15 years (mean 10 years, median 9.5 years). In fourteen patients the first clinical feature was cortical myoclonus, with reported symptoms of "tremor" or overt jerking. One patient (Case 3) presented with ataxia at age 3 and two patients presented with tremor and ataxia simultaneously (Cases 4 and 13). Three patients (Cases 14, 16 and 18) presented with a generalised tonic-clonic seizure (GTCS) at age 14, 9 and 12 years respectively, without prior recognition of myoclonus.

Seizures and other neurological findings

Patients experienced progressively severe and frequent myoclonus (Supplementary Video). Commonly initially reported as "tremor", the myoclonus was action-induced and often resulted in falls. In general, the myoclonus was reportedly worse in the mornings (Cases 5, 8, 12, 15, 16), in the context of stress, anxiety or startle (Cases 4, 5, 6, 10, 11, 19) and exacerbated during menses (Cases 8, 10, 12, 19). The parents of Case 14 denied she had myoclonus; however, on neurological examination at age 17 years myoclonus was clearly evident. This discrepancy was possibly due to the parents' unwillingness to accept that she had the same disorder that afflicted her older brother, mother and maternal aunt.

GTCS were rare and for Case 17 they were absent. GTCS were most frequent in teenage years. In Case 19, some convulsions were preceded by a sensation of stiffness and paraesthesia on the left leg, raising the possibility of a focal onset, but this was not consistent and her EEGs showed generalized epileptiform activity. Two patients had experienced earlier febrile seizures (Cases 14 and 15).

Ataxia was reported in 19/20 patients (Supplementary Table) and generally occurred early in the disease course. It was quickly overshadowed by myoclonus as the primary impediment to ambulation. Later in the course, the clinical distinction of incoordination due to cerebellar signs versus action myoclonus was difficult. Other neurological features, such as hearing loss, retinal abnormalities, sensory impairment, pyramidal or extrapyramidal signs, were not observed.

Surprisingly, family members reported transient improvement in gait and myoclonus with high fever in six patients (Supplementary Table). This typically lasted just hours or a few days while the patient was febrile. The mother of Case 8 stated adamantly "we should keep her sick!" when reflecting on her daughter's improved symptoms during fever. In addition, Case 17 noted improvement with alcohol, whilst Cases 11 and 19 both described marked improvement during pregnancy.

Cognitive function

There was notable preservation of cognition in the context of severe motor disability. In nine, where formal neuropsychological tests were done, verbal measures were in the low normal range. Myoclonus and ataxia prevented accurate assessment of non-verbal abilities requiring drawing, etc. Mild cognitive decline occurred in at least eleven patients (Supplementary Table), but severe dementia was not observed.

Clinical course

Nine patients were wheelchair bound and fully dependent by their late teenage years (Supplementary Table). Severe myoclonus was the predominant reason for loss of independent ambulation. The disorder appeared to be relatively stable in mid-adult life. Early death was not observed with nine patients being 30 years or older. The oldest patient (Case 20) died at age 63 years due to pneumonia with slowly progressive respiratory failure, that may have been contributed to by his neurological disability.

Therapy

At last evaluation, patients were on 1-5 anti-epileptic drugs (mean and median 3); two patients remained on monotherapy (valproate, n=1; topiramate, n=1). Systematic evaluation of efficacy was not possible but the clinical impression was that valproate was the most effective drug against myoclonus and remained a current medication for 15/18 patients in whom it had been trialled. Zonisamide was a current and successful medication for 8/9 patients who had trialled it; clonazepam for 12/16; levetiracetam for 6/12; acetazolamide 5/5; topiramate for 4/7 patients. Lamotrigine was trialled unsuccessfully in 5/6 patients resulting in worsening of myoclonus in three. The modified Atkins diet, ketogenic diet and a low-glycemic-index treatment were trialled unsuccessfully in a single patient each (Supplementary Table).

Electroencephalography and polygraphy

Source EEG data were available for eleven patients and showed relative preservation of background rhythms with generalized polyspike, polyspike-wave and sometimes spike-wave discharges (Fig 1A and B). Additional focal occipital epileptiform discharges were evident in Case 14. Photosensitivity was documented in 7/11 patients.

Myoclonic jerks were rare at rest but clearly activated with action. Polygraphic EEG-EMG recordings sporadically showed that brief paroxysms of polyspikes and wave occurred in association with positive-negative myoclonic jerks (Fig 1C). Action myoclonus was prominent, occurring incessantly during active movements without obvious EEG correlates and showing a quasi-rhythmic time course (Fig 1D and E). The evaluation of EEG-EMG relationship revealed a clear coherent peak in the beta band. The time transfer calculated between contralateral fronto-central EEG derivation and the activated muscle demonstrated a time lag (mean 13.7 ms, range 12.2-14.9 ms) consistent with fast cortico-spinal transfer of the cortical activity (Fig 1F). Enlarged or "giant" somatosensory evoked potentials (N20-P25 ranging from 13.5 to 28.2 μV) and enhanced C reflexes further documented the pathological cortical excitability associated with cortical-reflex myoclonus.

Brain magnetic resonance imaging

MRIs were available for eleven patients at ages 8-44 years. These revealed global symmetrical cerebellar atrophy, usually of moderate severity, an enlarged 4th ventricle and a prominent corpus callosum (Fig 2).

Serial MRI studies were available for two patients. Imaging of Case 11 showed deterioration from mild cerebellar atrophy at age 16 (Fig 3A) to moderate cerebellar atrophy at age 44 (Fig 3B). The scans of Case 12 showed minimal change between the ages of 23 and 39 years; moderate to severe cerebellar atrophy seen on both. The appearance of the prominent corpus callosum did not change in either subject.

In vitro analysis of channel properties

To assess the functional effects of the p.R320H substitution on human $K_V3.1^{WT}$ channel function in the mammalian HEK293 expression system, we used automated-planar

patch-clamp technology in the whole-cell configuration at 27 ^{o}C. Potassium currents were recorded from stably transfected HEK293 cells expressing $K_V3.1^{WT}$ alone or with transiently co-transfected mutant $K_V3.1^{R320H}$ ($K_V3.1^{WT+R320H}$). Representative current family traces acquired from $K_V3.1^{WT}$ channel illustrate robust voltage activated currents (Fig 4A, left panel). Co-expression of $K_V3.1^{WT}$ channel with $K_V3.1^{R320H}$ resulted in a significant reduction of the peak current amplitude, an effect previously reported in the *Xenopus* oocyte expression system [14] (Fig 4A right panel, Figs 4B, 4C). Figure 4D examines the voltage-dependence of activation of $K_V3.1^{WT}$ channels and $K_V3.1^{WT+R320H}$ channels at 27 ^{o}C. Data points were fit with a Boltzmann equation and the voltage-dependence of half-activation ($V_{0.5}$) and slope values were obtained. R320H substitution caused a hyperpolarizing shift in the voltage-dependence of activation compared to the $K_V3.1^{WT}$ channel, which is reflected in the significant change in the $V_{0.5}$ value (Fig 4E). The mutation had no effect on the slope of the conductance curve.

The observation of improvement in clinical symptoms for some patients with fever led us to examine channel properties at higher temperatures. We used 36 ^{o}C to reflect body temperature and 39 ^{o}C as the febrile temperature. Visual inspection of representative current family traces, illustrate how increases in temperature to 36 ^{o}C and 39 ^{o}C have a profound effect on $K_V3.1^{WT}$ channel properties (Fig 5A top panel), with the appearance of a delayed inactivation resulting in a significantly lower steady state current. Interestingly, this temperature-dependent effect was not observed with $K_V3.1^{WT+R320H}$ channels, showing only minor alterations of inactivation (Fig 5A bottom panel). For all temperatures studied, peak currents for $K_V3.1^{WT+R320H}$ were significantly reduced at potentials > +50 mV compared to the WT (Fig 5B).

Figure 6 shows the effects of temperature on the voltage-dependence of activation obtained from peak currents of cells expressing either $K_V3.1^{WT}$ alone or $K_V3.1^{WT+R320H}$ channels. Data points were fitted with a Boltzmann equation and the $V_{0.5}$ and slope values were obtained (slope data not shown). We observed a significant hyperpolarising shift in the voltage-dependence of activation for the $K_V3.1^{WT+R320H}$ compared to $K_V3.1^{WT}$ at all temperatures (Fig 6A). In addition, the change in $V_{0.5}$ was significantly different between the 27 ^{o}C and 39 ^{o}C for both $K_V3.1^{WT+R320H}$ and $K_V3.1^{WT}$, but reached significance (p<0.05) only for the WT when the temperature was elevated from 36 ^{o}C to 39 ^{o}C (Fig 6B).

In Figure 7, averaged traces of currents recorded at +80 mV and normalised to peak illustrate the striking temperature-dependent changes in $K_V3.1^{WT}$ channel kinetics as the temperature is elevated from 27 ^oC to 36 ^oC or 39 ^oC (Fig 7A top panel). This effect was not as marked for cells expressing $K_V3.1^{WT+R320H}$ channels (Fig 7A bottom panel). Changes in channel kinetics were quantified as area under the curve (AUC) as a marker of extent of inactivation. Highly significant reductions in AUC were observed for $K_V3.1^{WT}$ channels as temperature was raised from 27 ^oC to 36 ^oC or 39 ^oC (Fig 7B). However, for cells expressing $K_V3.1^{WT+R320H}$, the AUC decreased significantly only as the temperature was raised from 27 ^oC to 39 ^oC, but not 36 ^oC (Fig 7C). When the AUC for $K_V3.1^{WT}$ channels was compared to the AUC for $K_V3.1^{WT+R320H}$ channels, significant differences were observed at all temperatures studied (Fig 7D).

We note that the $V_{0.5}$ comparisons that did not show significant differences were underpowered due to high variance in the data. The prohibitively high n-values required to increase power precluded further analysis. In contrast, the non-significant comparisons in AUC values for the mutant were higher powered at 80% (27°C to 36°C) and 50% (36°C to 39°C).

Discussion

MEAK has a homogeneous clinical presentation; the age of onset and clinical features are remarkably similar to ULD [17-19], despite the clear genetic and biological differences (Table 1). Rapid early disease progression was evident, with incessant myoclonus resulting in wheelchair dependency by mid teenage, in approximately half of MEAK patients, which represents a somewhat more severe progression than ULD. Furthermore, and similar to ULD, the progressive nature of MEAK appears to stabilize in adulthood and does not result in early death. This is a distinguishing factor from many other PME syndromes, including some that resemble ULD at onset and lack progressive dementia. For example, in North Sea PME and AMRF, due to recessive mutations in *GOSR2* [5] and *SCARB2* [20] respectively, death typically occurs by the fourth decade of life [21, 22].

Generalized tonic-clonic seizures were usually infrequent in MEAK and, apart from the action myoclonus and ataxia, there were no other consistent neurological features. Cognitive impairment was hard to quantitate in patients with severe action myoclonus, and was further confounded by effects of anti-epileptic drugs and by limited schooling in many cases due to the disability. About half the patients appeared to have some slow cognitive decline after disease onset but, unlike PME due to Lafora disease and the neuronal ceroid lipofuscinoses [1], relentless dementia was not observed.

Treatment was challenging and our retrospective evaluation precluded systematic assessment. Valproate, zonisamide, clonazepam and levetiracetam were the drugs that appeared to be most effective, whereas lamotrigine appeared to exacerbate the myoclonus. Tonic-clonic seizures were generally well controlled, but the effect of drugs on action myoclonus was modest.

Neurophysiological investigations showed a cortical origin of the myoclonic phenomena (Fig 1). Spontaneous myoclonic jerks associated with polyspike and wave paroxysms were rare. Action myoclonus with a quasi-rhythmic time course was prominent; coherence analysis revealed an EEG correlate to the myoclonic bursts, while phase analysis indicated a direct cortico-spinal transfer of the EEG oscillatory activity (Fig 1F). This latter finding is consistent with the hypothesis that this type of

myoclonus is due to an exaggeration of the physiological cortical drive to muscle that subserves voluntary contractions in healthy subjects [23]. A loss of intracortical inhibition resulting in motor cortex hyperexcitability has been postulated to underlie the susceptibility to generate rhythmic myoclonic activity in PMEs [24]. Giant SEPs and enhanced C reflexes further demonstrated that the cortex was hyperexcitable [25].

Action and reflex myoclonus can be seen in other PMEs, but the remarkable rhythmicity captured on EEG/EMG, resembling a "cortical tremor" [26] and completely substituting normal muscle contraction seen in MEAK patients, is not as common [23, 27, 28]. As has been suggested for other myoclonic conditions, the synchronized discharges of pyramidal neurons transferred through the pyramidal tract to the peripheral motor system result in synchronous motor unit discharges that lead to rhythmic myoclonic jerks, rather than normal integrated movements [29]. This striking co-activation of agonist and antagonist muscles, perhaps explains the marked gait instability of MEAK patients (Fig 1E and Supplementary Video).

Visible cerebellar atrophy on MRI appeared to start by clinical disease onset, progressed over the teenage years and into early adulthood but then possibly plateau, consistent with the clinical finding of relative disease stability in adulthood. The observed prominent and occasionally thick corpus callosum across patients suggests this may be an important brain imaging feature of MEAK, perhaps reflecting an underlying axonal guidance abnormality [30].

The majority of MEAK patients were from European countries; this likely reflects ascertainment bias. There was no geographical clustering as is seen in other PMEs, such as ULD and North Sea PME that follow recessive inheritance. ULD is common in countries around the Baltic Sea, with an incidence of 1/20,000 in Finland [31]. ULD is also common in other founder populations in both North Africa and North America. Similarly, all known patients with *GOSR2* mutation derive from countries surrounding the North Sea [22]. With MEAK typically arising from *de novo* mutation, the distribution of cases should be independent of population geography.

We previously reported the estimated mutation rate of c.959G>A in *KCNC1* as 1.75×10^{-7} mutations per person, which is equal to 1 mutation in every 5,700,000 conceptions [14]. This rate is typical for mutations occurring at CpG dinucleotide sites [32] and suggests

that the mutation potentially affects hundreds of people worldwide. Consistent with this, six of our unrelated cases were recruited through a multi-center clinical collaboration in Italy [2]; based on the estimated mutation rate and Italy's population, the total number of MEAK patients in Italy should be close to ten.

Paternal age is important to disease risk in many conditions due to *de novo* mutation [32]. We attempted to determine the parent-of-origin of the mutations in our cohort, but the paucity of SNPs in *KCNC1* and issues with DNA quality prevented definitive analysis. The data on parental age did not demonstrate a clear trend to older fathers.

While *de novo* mutation accounted for the majority of patients, we reported a second autosomal dominant family. This highlights the importance of exploring patient family histories. Genetic counselling is important for both *de novo* and familial cases as the degree of incapacity in MEAK does not necessarily preclude partnering, apparent sporadic cases can be due to gonadal mosaicism, and the genetic risks to siblings and offspring are very different from those for ULD and other recessive PMEs.

Although the clinical phenotype of MEAK is relatively homogeneous, the severity does vary, and the full spectrum may not yet be appreciated. The original *KCNC1* molecular genetic discovery [14] was made in a cohort of unsolved PME cases. Four new patients were subsequently identified and perhaps importantly one of these patients (Case 17) had not reported any GTCS (Supplementary Table). As opposed to PMEs seen by epileptologists, movement disorder specialists often see patients with myoclonus and progressive ataxia but without GTCS: a clinical presentation known as progressive myoclonic ataxia (PMA). This difference in referral patterns for the PMAs versus the PMEs may mean we have yet to characterize the full phenotypic spectrum. That the PMEs and PMAs may share common genetic causes has long been appreciated [33]; recently this clinical overlap has been highlighted for *GOSR2* [34].

That *KCNC1* mutation could have a PMA presentation is supported by the observation that dominant mutations in *KCNC3*, encoding $K_V3.3$ from the same K^+ channel subfamily, cause spinocerebellar ataxia (SCA13) [35]. The phenotypic spectrum of SCA13 is broad with onset age ranging from infancy to 60 years [36]. Like MEAK, however, life span is not shortened, assistance with gait is required as the disease progresses and MRI studies show progressive cerebellar atrophy with disease duration

[37-39]. Interestingly, there have been rare SCA13 cases associated with seizures [36-38, 40]; however, myoclonus is not reported. So although *KCNC3* and *KCNC1* are from the same K_V3 subfamily, this would suggest they present somewhat distinctly. Despite this, further exploration of a predominantly ataxia presentation for *KCNC1* and a seizure presentation for *KCNC3* warrants further exploration.

$K_V3.1$ is activated at depolarisations more positive than -40 mV. On repolarization of the membrane, $K_V3.1$ channels deactivate rapidly, making them well suited to their role in maintaining high-frequency neuronal firing [41]. Importantly, these channels are expressed predominantly in interneurons [41-43] with dominant negative mutations likely resulting in disinhibition and consequent neuronal network hyper-excitability [14]. The overall effect of the R320H mutation on neuronal excitability is difficult to predict intuitively from two opposing biophysical changes observed both in *Xenopus* oocytes and HEK293 cells. Reduced current levels in the presence of the mutation would lead to a loss of function and potential disinhibition [41], albeit tempered somewhat by the concomitant hyperpolarising shift in the activation voltage. Furthermore, $K_V3.1$ is expressed in adult neural precursor cells (NPCs). It has been shown that its knockdown significantly decreased NPC proliferation and their differentiation into neuroblasts [44]. This potential effect on neuronal plasticity may be an additional pathology related to R320H. Interestingly, Kv3.1 is reduced in brains of subjects with untreated schizophrenia and appears to be normalized with anti-psychotic drugs [45]. Mouse models should help to reveal the detailed neurophysiological mechanisms, including the overall impact on interneuron and pyramidal neuron function.

To explore the molecular mechanism of alleviation of disease symptoms at elevated body temperature observed in some MEAK patients, we measured channel properties at 36 ^{o}C and 39 ^{o}C. Earlier work has shown that hERG (human *ether-à-go-go-related gene*), $K_V2.1$ (*KCNB1*) and $K_V4.3$ (*KCND3*) have temperature sensitivity [46, 47]. No such data could be found for $K_V3.1$ channels and here we show that elevated temperature causes a hyperpolarising shift in the voltage dependence of activation and an increase in the rate of inactivation in the wild type channel. Interestingly, for both parameters the mutant channels showed blunted changes with elevated temperature.

With respect to the mechanism underlying alleviation of symptoms with temperature the most parsimonious explanation is that the hyperpolarising shift in the activation voltage of channels comprised only of WT subunits would be beneficial. The precise number of such channels *in vivo* is difficult to predict, but is expected to be approximately 6% assuming equal expression of WT and mutant alleles. A left shift in this residuum of WT only channels will result in increased current magnitude that would directly counter the reduced currents seen in mutant channels. The blunted temperature dependent inactivation seen in the mutant channels may also contribute by maintaining channel availability during elevations in temperature. Thus, in patients harbouring mutant subunits, temperature dependent improvement of symptoms could be due to increased availability of WT only channels in combination with the maintenance of the availability of mutant channels. A net increase in $K_V3.1$ channel availability would enhance the ability of interneuron firing and consequently reduce network excitability.

Further studies in more complex experimental and simulation models are needed to clarify the precise biological mechanisms. This study was limited by its retrospective nature, particularly in that it did not allow for more objective clinical measures in response to fever. The possibility for earlier molecular genetic diagnosis now makes this more feasible. This and other experimental work into the mechanisms of *KCNC1* hold promise for MEAK patients, with the ion channel defect a potential target for precision therapy in the future.

Acknowledgements

We would like to thank the patients and their families for their participation. We acknowledge and thank Dr Anna Potulska-Chromik (Department of Neurology, Medical University of Warsaw, Warsaw, Poland) and Dr Robert Szymanczak (Genomed SA, Ponczowa 12, Warsaw, Poland) for their contribution to data acquisition.

SFB was supported by National Health and Medical Research Council Program Grant (ID: 628952); SM and HL received support from the German Network for Rare Diseases of the Federal Ministry of Education and Research (BMBF: IonNeurONet 01GM1105A) and the EuroEPINOMICS program of the European Science Foundation (DFG grant Le1030/11-1). FB, LL, PT thank Telethon foundation (grant GGP 13200 to P.T.) for financial support. A-EL was supported by the Folkhälsan Research Foundation, Helsinki, Finland. MM was supported by Doctoral Programme of Biomedicine, Emil Aaltonen Foundation, University of Helsinki Funds, Epilepsy Research Foundation, Arvo and Lea Ylppö Foundation, Finnish Brain Foundation, Paulo Foundation and Biomedicum Helsinki Foundation.

Author contributions

Conception and design of the study: S.F.B., S.P., K.L.O. Acquisition and analysis of data: K.L.O., S.F., C.J.M., M.M., S.A.M., L.C., A.M.B-C., A.K., F.B., C.D., F.R., R.M., B.B-Z., R.S., F.P., J.M., D.F., A.C., B.A.E., F.A., E.A., K.S., A.L-B., P.R., E.P., P.T., L.L., E.G., M.L., A.W., R.S.M., F.B., Z.A., G.R., C.A.R., S.M., H.L., A-E.L., S.P., S.F.B. Drafting the manuscript or figures: K.L.O., S.F., C.J.M., S.A.M., A-E.L., S.P., S.F.B.

Potential Conflicts of Interest

Nothing to report.

References

1. Berkovic SF, Andermann F, Carpenter S, Wolfe LS. Progressive myoclonus epilepsies: specific causes and diagnosis. N Engl J Med 1986;315:296-305

2. Franceschetti S, Michelucci R, Canafoglia L, et al. Progressive myoclonic epilepsies: definitive and still undetermined causes. Neurology 2014;82:405-411

3. Canafoglia L, Robbiano A, Pareyson D, et al. Expanding sialidosis spectrum by genome-wide screening: NEU1 mutations in adult-onset myoclonus. Neurology 2014;82:2003-2006

4. Dibbens LM, Michelucci R, Gambardella A, et al. SCARB2 mutations in progressive myoclonus epilepsy (PME) without renal failure. Ann Neurol 2009;66:532-536

5. Corbett MA, Schwake M, Bahlo M, et al. A mutation in the Golgi Qb-SNARE gene GOSR2 causes progressive myoclonus epilepsy with early ataxia. Am J Hum Genet 2011;88:657-663

6. Park JK, Orvisky E, Tayebi N, et al. Myoclonic epilepsy in Gaucher disease: genotype-phenotype insights from a rare patient subgroup. Pediatr Res 2003;53:387-395

7. DiMauro S, Schon EA, Carelli V, Hirano M. The clinical maze of mitochondrial neurology. Nat Rev Neurol 2013;9:429-444

8. Koide R, Ikeuchi T, Onodera O, et al. Unstable expansion of CAG repeat in hereditary dentatorubral-pallidoluysian atrophy (DRPLA). Nat Genet 1994;6:9-13

9. Nance MA, Myers RH. Juvenile onset Huntington's disease--clinical and research perspectives. Ment Retard Dev Disabil Res Rev 2001;7:153-157

10. Takao M, Benson MD, Murrell JR, et al. Neuroserpin mutation S52R causes neuroserpin accumulation in neurons and is associated with progressive myoclonus epilepsy. J Neuropathol Exp Neurol 2000;59:1070-1086

11. Noskova L, Stranecky V, Hartmannova H, et al. Mutations in DNAJC5, encoding cysteine-string protein alpha, cause autosomal-dominant adult-onset neuronal ceroid lipofuscinosis. Am J Hum Genet 2011;89:241-252

12. Afawi Z, Oliver KL, Kivity S, et al. Multiplex families with epilepsy: Success of clinical and molecular genetic characterization. Neurology 2016;86:713-722

13. Genton P, Delgado-Escueta A, Serratosa JM, Bureau M. Progressive Myoclonus Epilepsies. In: Bureau M, Genton P, Dravet C, Delgado-Escueta A, Tassinari CA, Thomas P, Wolf P, editors. Epileptic Syndromes in Infancy, Childhood and Adolescence: John Libbey Eurotext Ltd; 2012:575-606

14. Muona M, Berkovic SF, Dibbens LM, et al. A recurrent de novo mutation in KCNC1 causes progressive myoclonus epilepsy. Nat Genet 2015;47:39-46

15. Panzica F, Canafoglia L, Franceschetti S, et al. Movement-activated myoclonus in genetically defined progressive myoclonic epilepsies: EEG-EMG relationship estimated using autoregressive models. Clin Neurophysiol 2003;114:1041-1052

16. Cruccu G, Aminoff MJ, Curio G, et al. Recommendations for the clinical use of somatosensory-evoked potentials. Clin Neurophysiol 2008;119:1705-1719

17. Genton P, Michelucci R, Tassinari CA, Roger J. The Ramsay Hunt syndrome revisited: Mediterranean myoclonus versus mitochondrial encephalomyopathy with ragged-red fibers and Baltic myoclonus. Acta Neurol Scand 1990;81:8-15

18. Magaudda A, Ferlazzo E, Nguyen VH, Genton P. Unverricht-Lundborg disease, a condition with self-limited progression: long-term follow-up of 20 patients. Epilepsia 2006;47:860-866

19. Hypponen J, Aikia M, Joensuu T, et al. Refining the phenotype of Unverricht-Lundborg disease (EPM1): a population-wide Finnish study. Neurology 2015;84:1529-1536

20. Berkovic SF, Dibbens LM, Oshlack A, et al. Array-based gene discovery with three unrelated subjects shows SCARB2/LIMP-2 deficiency causes myoclonus epilepsy and glomerulosclerosis. Am J Hum Genet 2008;82:673-684

21. Badhwar A, Berkovic SF, Dowling JP, et al. Action myoclonus-renal failure syndrome: characterization of a unique cerebro-renal disorder. Brain 2004;127:2173-2182

22. Boisse Lomax L, Bayly MA, Hjalgrim H, et al. 'North Sea' progressive myoclonus epilepsy: phenotype of subjects with GOSR2 mutation. Brain 2013;136:1146-1154

23. Brown P, Farmer SF, Halliday DM, Marsden J, Rosenberg JR. Coherent cortical and muscle discharge in cortical myoclonus. Brain 1999;122 (Pt 3):461-472

24. Valzania F, Strafella AP, Tropeani A, Rubboli G, Nassetti SA, Tassinari CA. Facilitation of rhythmic events in progressive myoclonus epilepsy: a transcranial magnetic stimulation study. Clin Neurophysiol 1999;110:152-157

25. Kakigi R, Shibasaki H. Generator mechanisms of giant somatosensory evoked potentials in cortical reflex myoclonus. Brain 1987;110 (Pt 5):1359-1373

26. Ikeda A, Kakigi R, Funai N, Neshige R, Kuroda Y, Shibasaki H. Cortical tremor: a variant of cortical reflex myoclonus. Neurology 1990;40:1561-1565

27. Canafoglia L, Bugiani M, Uziel G, et al. Rhythmic cortical myoclonus in Niemann-Pick disease type C. Mov Disord 2006;21:1453-1456

28. Rubboli G, Franceschetti S, Berkovic SF, et al. Clinical and neurophysiologic features of progressive myoclonus epilepsy without renal failure caused by SCARB2 mutations. Epilepsia 2011;52:2356-2363

29. Brown P. Abnormal oscillatory synchronisation in the motor system leads to impaired movement. Curr Opin Neurobiol 2007;17:656-664

30. Merlini L, Anooshiravani M, Kanavaki A, Hanquinet S. Microstructural changes in thickened corpus callosum in children: contribution of magnetic resonance diffusion tensor imaging. Pediatr Radiol 2015;45:896-901

31. Koskiniemi ML. Baltic myoclonus. Adv Neurol 1986;43:57-64

32. Kong A, Frigge ML, Masson G, et al. Rate of de novo mutations and the importance of father's age to disease risk. Nature 2012;488:471-475

33. Marsden CD, Harding AE, Obeso JA, Lu CS. Progressive myoclonic ataxia (the Ramsay Hunt syndrome). Arch Neurol 1990;47:1121-1125

34. van Egmond ME, Verschuuren-Bemelmans CC, Nibbeling EA, et al. Ramsay Hunt syndrome: clinical characterization of progressive myoclonus ataxia caused by GOSR2 mutation. Mov Disord 2014;29:139-143

35. Waters MF, Minassian NA, Stevanin G, et al. Mutations in voltage-gated potassium channel KCNC3 cause degenerative and developmental central nervous system phenotypes. Nat Genet 2006;38:447-451

36. Figueroa KP, Minassian NA, Stevanin G, et al. KCNC3: phenotype, mutations, channel biophysics-a study of 260 familial ataxia patients. Hum Mutat 2010;31:191-196

37. Herman-Bert A, Stevanin G, Netter JC, et al. Mapping of spinocerebellar ataxia 13 to chromosome 19q13.3-q13.4 in a family with autosomal dominant cerebellar ataxia and mental retardation. Am J Hum Genet 2000;67:229-235

38. Stevanin G, Durr A, Benammar N, Brice A. Spinocerebellar ataxia with mental retardation (SCA13). Cerebellum 2005;4:43-46

39. Subramony SH, Advincula J, Perlman S, et al. Comprehensive phenotype of the p.Arg420his allelic form of spinocerebellar ataxia type 13. Cerebellum 2013;12:932-936

40. Figueroa KP, Waters MF, Garibyan V, et al. Frequency of KCNC3 DNA variants as causes of spinocerebellar ataxia 13 (SCA13). PLoS One 2011;6:e17811

41. Rudy B, McBain CJ. Kv3 channels: voltage-gated K+ channels designed for high-frequency repetitive firing. Trends Neurosci 2001;24:517-526

42. Chow A, Erisir A, Farb C, et al. K(+) channel expression distinguishes subpopulations of parvalbumin- and somatostatin-containing neocortical interneurons. J Neurosci 1999;19:9332-9345

43. Weiser M, Bueno E, Sekirnjak C, et al. The potassium channel subunit KV3.1b is localized to somatic and axonal membranes of specific populations of CNS neurons. J Neurosci 1995;15:4298-4314

44. Yasuda T, Cuny H, Adams DJ. Kv3.1 channels stimulate adult neural precursor cell proliferation and neuronal differentiation. J Physiol 2013;591:2579-2591

45. Yanagi M, Joho RH, Southcott SA, Shukla AA, Ghose S, Tamminga CA. Kv3.1-containing K(+) channels are reduced in untreated schizophrenia and normalized with antipsychotic drugs. Mol Psychiatry 2014;19:573-579

46. Vandenberg JI, Varghese A, Lu Y, Bursill JA, Mahaut-Smith MP, Huang CL. Temperature dependence of human ether-a-go-go-related gene K+ currents. Am J Physiol Cell Physiol 2006;291:C165-175

47. Yang F, Zheng J. High temperature sensitivity is intrinsic to voltage-gated potassium channels. Elife 2014;3:e03255

Figure legends

Fig 1. Electoencephalography and polygraphy in MEAK patients.

EEG-EMG recordings showing brief paroxysms of irregular spike-waves during awake recording (A, Case 9) and polyspikes (similar to those associated with spontaneous myoclonus) occurring during light sleep (B, Case 9). Polygraphic recording showing spontaneous positive-negative myoclonic jerks associated with isolated polyspikes (C) in Cases 18 (left) and 9 (right). Polygraphy showing intense action myoclonus during left hand isometric extension, without obvious EEG correlates in Case 18 (D). Magnification of action myoclonus (E) showing remarkably similar near-rhythmic persistent jerks in Cases 18 (top), 7 (middle) and 9 (bottom). Cortico-muscular coherence spectrum (F) shows a coherence peak at about 20 Hz while the phase slope indicates a cortico-muscular transfer of 14.1 ms (Case 9) for the forearm, consistent with conduction from the cortex via the pyramidal pathway.

Fig 2. Brain MRIs.

(A) Sagittal images of 3 patients showing prominent corpus callosum with similar morphology. Cerebellar atrophy particularly affecting the superior vermis is also evident. (B) Coronal images showing moderate/severe atrophy of the cerebellar hemispheres with ex-vacuo dilation of the 4th ventricles.

Fig 3. Serial brain MRIs for Case 11 demonstrating progression of cerebellar atrophy.

Midline sagittal T1 weighted scans for Case 11 at ages 16 (A) and 44 (B) years demonstrating considerable interim deterioration from minor to moderate cerebellar atrophy with increased prominence of cerebellar folia. Some cerebral atrophy is also apparent.

Fig 4. Functional analysis of the $K_V3.1^{R320H}$ substitution in $K_V3.1^{WT}$ at 27 ^oC. (A) Representative current traces obtained from HEK293 cells stably expressing $K_V3.1^{WT}$ and stably expressing $K_V3.1^{WT}$ with transiently expressed $K_V3.1^{R320H}$ ($K_V3.1^{WT+R320H}$). Cells were held at -80 mV and stepped, in 10 mV increments, to +80 mV for 2 s, every 7 s. Scale bars apply to all traces. (B) Average peak current-voltage relationship curves for $K_V3.1^{WT}$ (●) and $K_V3.1^{WT+R320H}$ (□) channels. (C) Comparison of the average normalised currents at +80 mV for the two experimental groups, $K_V3.1^{WT}$ (solid bars) and $K_V3.1^{WT+R320H}$ (open bars), shown with S.E.M. (D) Voltage-dependence of

normalised peak conductance shown for $K_V3.1^{WT}$ (●) and $K_V3.1^{WT+R320H}$ (□) as a function of voltage. Boltzmann curves were fit to pooled averages. (E) Comparison of the average voltage of half activation ($V_{0.5}$) for $K_V3.1^{WT}$ (solid bars) and $K_V3.1^{WT+R320H}$ (open bars). $K_V3.1^{WT}$ (n = 45) and $K_V3.1^{WT+R320H}$ (n = 41). Statistical significance marked as ** p<0.01; **** p<0.0001.

Fig 5. Effect of increased temperature on $K_V3.1^{WT}$ and $K_V3.1^{WT+R320H}$ mutant channels. (A) Representative current family traces, for $K_V3.1^{WT}$ (top panel) and $K_V3.1^{WT+R320H}$ (bottom panel) at 27 ^oC (black), 36 ^oC (blue) and 39 ^oC (pink). Scale bars apply to all traces. (B) Average peak current-voltage relationship curves for $K_V3.1^{WT}$ (●) and $K_V3.1^{WT+R320H}$ (□) at 27 ^oC (black), 36 ^oC (blue) and 39 ^oC (pink). $K_V3.1^{WT}$ (n = 45), 36 ^oC (n = 25) and 39 ^oC (n = 20) and $K_V3.1^{WT+R320H}$ channels 27 ^oC (n = 41), 36 ^oC (n = 19) and 39 ^oC (n = 14). Statistical significance marked as ** p<0.01; *** p<0.001; **** p<0.0001.

Fig 6. Temperature dependent effects on channel conductance. (A) Voltage-dependence of normalised peak conductance shown for $K_V3.1^{WT}$ (●) and $K_V3.1^{WT+R320H}$ (□) as a function of voltage at 27 ^oC (black), 36 ^oC (blue) and 39 ^oC (pink). Boltzmann curves were fit to pooled averages. (B) Comparison of the average voltage of half activation ($V_{0.5}$) for $K_V3.1^{WT}$ (solid bars) and $K_V3.1^{WT+R320H}$ (open bars) at 27 ^oC (black), 36 ^oC (blue) and 39 ^oC (pink). $K_V3.1^{WT}$ channels 27 ^oC (n = 45), 36 ^oC (n = 25) and 39 ^oC (n = 20) and $K_V3.1^{WT+R320H}$ channels 27 ^oC (n = 41), 36 ^oC (n = 19) and 39 ^oC (n = 14). Statistical significance marked as * p<0.05; ** p<0.01; *** p<0.001.

Fig 7 Temperature dependent effects on channel inactivation. (A) Mean of current traces recorded at +80 mV and normalised to the peak current for $K_V3.1^{WT}$ (top panel) and $K_V3.1^{WT+R320H}$ (bottom panel) at 27 ^oC (black), 36 ^oC (blue) and 39 ^oC (pink). Scale bar applies to all traces. (B) Inactivation for $K_V3.1^{WT}$ was quantified as area under the curve (AUC) at 27 ^oC (solid black), 36 ^oC (solid blue) and 39 ^oC (solid pink). (C) Inactivation for $K_V3.1^{WT+R320H}$ was quantified as AUC at 27 ^oC (open black), 36 ^oC (open blue) and 39 ^oC (open pink). (D) Comparison of AUC values for $K_V3.1^{WT}$ (solid bars) and $K_V3.1^{WT+R320H}$ (open bars) at 27 ^oC (black), 36 ^oC (blue) and 39 ^oC (pink). All AUC values were calculated from panel A. $K_V3.1^{WT}$ channels 27 ^oC (n = 45), 36 ^oC (n = 25) and 39 ^oC (n = 20) and $K_V3.1^{WT+R320H}$ channels 27 ^oC (n = 41), 36 ^oC (n = 19) and

39 ^{o}C (n = 14). Statistical significance marked as ** p<0.01; *** p<0.001; **** p<0.0001.

Supplementary material

Supplementary Table. MEAK progressive myoclonus epilepsy clinical characteristics and seizure types in 20 patients.

Supplementary Video. Video of Case 17 highlighting the debilitating upper-limb myoclonus and gait difficulties faced by MEAK patients due to both myoclonus and ataxia.

Table 1. Comparison of typical MEAK characteristics to classical Unverricht-Lundborg disease (ULD).

	MEAK	ULD [17, 18]
First symptom	Myoclonus (or "tremor")	Tonic-clonic seizures or myoclonus
Disease onset: mean	10 years	11 years
Disease onset: range	3-15 years	6-16 years
Progressive features	Myoclonus, ataxia	Myoclonus, ataxia
Cognitive decline	Mild or absent	Mild or absent
Mode of inheritance	Autosomal dominant Usually *de novo*	Autosomal recessive May cluster due to founder effect (eg Finland)
Gene	*KCNC1*	*CSTB*
Protein function	Ion channel	Protease inhibitor

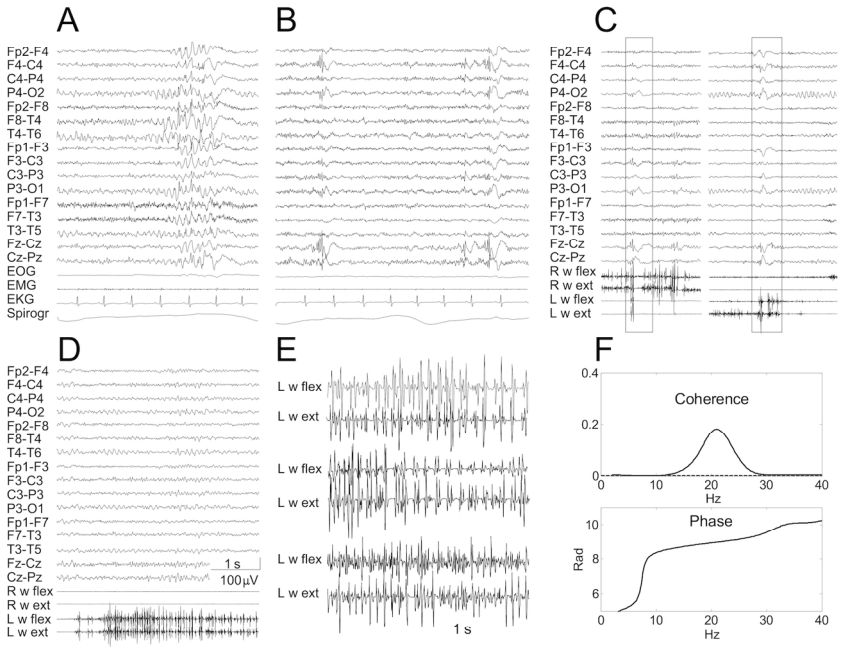

Electoencephalography and polygraphy in MEAK patients.EEG-EMG recordings showing brief paroxysms of irregular spike-waves during awake recording (A, Case 9) and polyspikes (similar to those associated with spontaneous myoclonus) occurring during light sleep (B, Case 9). Polygraphic recording showing spontaneous positive-negative myoclonic jerks associated with isolated polyspikes (C) in Cases 18 (left) and 9 (right). Polygraphy showing intense action myoclonus during left hand isometric extension, without obvious EEG correlates in Case 18 (D). Magnification of action myoclonus (E) showing remarkably similar near-rhythmic persistent jerks in Cases 18 (top), 7 (middle) and 9 (bottom). Cortico-muscular coherence spectrum (F) shows a coherence peak at about 20 Hz while the phase slope indicates a cortico-muscular transfer of 14.1 ms (Case 9) for the forearm, consistent with conduction from the cortex via the pyramidal pathway.

Fig 1

170x131mm (300 x 300 DPI)

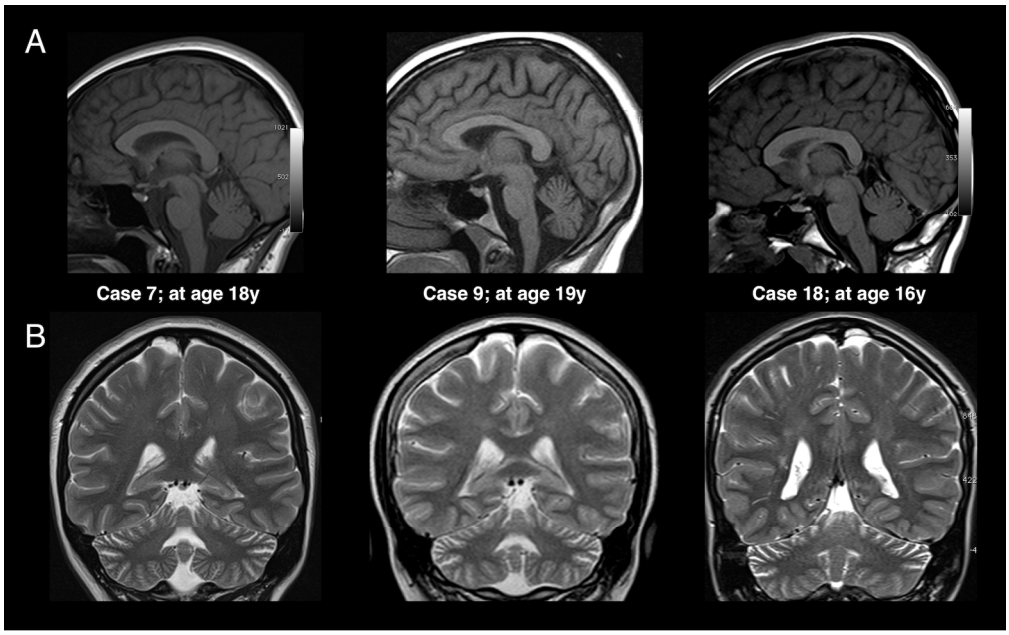

Brain MRIs. (A) Sagittal images of 3 patients showing prominent corpus callosum with similar morphology. Cerebellar atrophy particularly affecting the superior vermis is also evident. (B) Coronal images showing moderate/severe atrophy of the cerebellar hemispheres with ex-vacuo dilation of the 4th ventricles.
Fig 2
170x106mm (300 x 300 DPI)

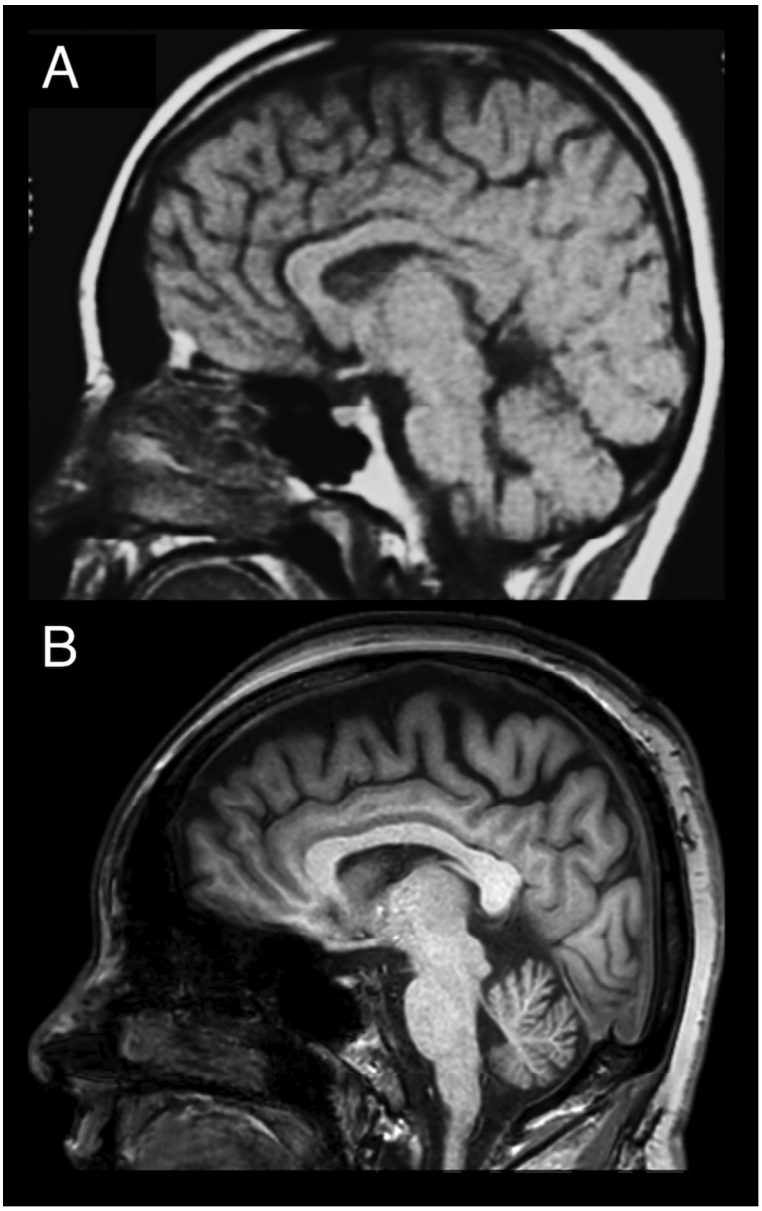

Serial brain MRIs for Case 11 demonstrating progression of cerebellar atrophy.Midline sagittal T1 weighted scans for Case 11 at ages 16 (A) and 44 (B) years demonstrating considerable interim deterioration from minor to moderate cerebellar atrophy with increased prominence of cerebellar folia.
Fig 3
80x127mm (300 x 300 DPI)

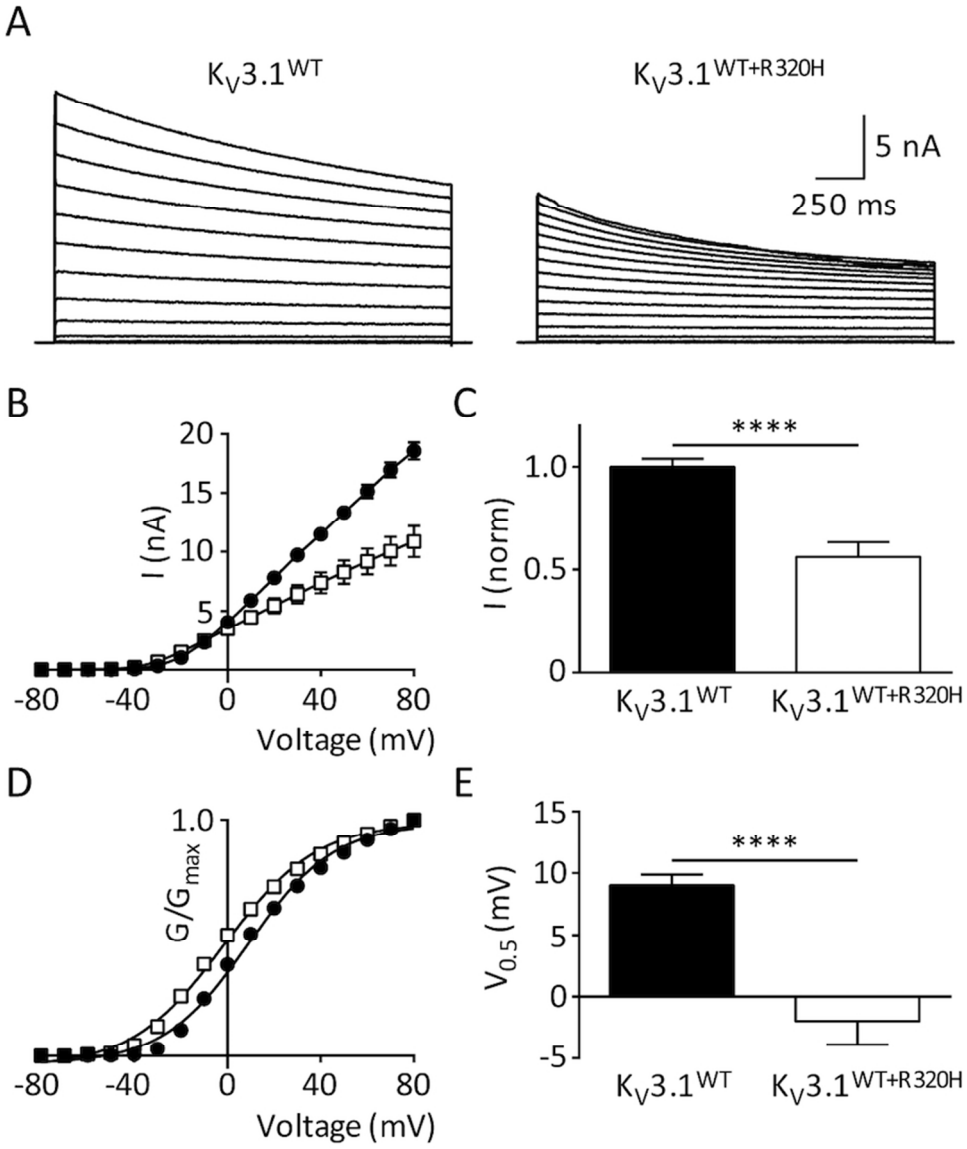

Functional analysis of the KV3.1R320H substitution in KV3.1WT at 27 oC. (A) Representative current traces obtained from HEK293 cells stably expressing KV3.1WT and stably expressing KV3.1WT with transiently expressed KV3.1R320H (KV3.1WT+R320H). Cells were held at -80 mV and stepped, in 10 mV increments, to +80 mV for 2 s, every 7 s. Scale bars apply to all traces. (B) Average peak current-voltage relationship curves for KV3.1WT () and KV3.1WT+R320H () channels. (C) Comparison of the average normalised currents at +80 mV for the two experimental groups, KV3.1WT (solid bars) and KV3.1WT+R320H (open bars), shown with S.E.M. (D) Voltage-dependence of normalised peak conductance shown for KV3.1WT () and KV3.1WT+R320H () as a function of voltage. Boltzmann curves were fit to pooled averages. (E) Comparison of the average voltage of half activation (V0.5) for KV3.1WT (solid bars) and KV3.1WT+R320H (open bars). KV3.1WT (n = 45) and KV3.1WT+R320H (n = 41). Statistical significance marked as ** $p<0.01$; **** $p<0.0001$.

Fig 4
80x91mm (300 x 300 DPI)

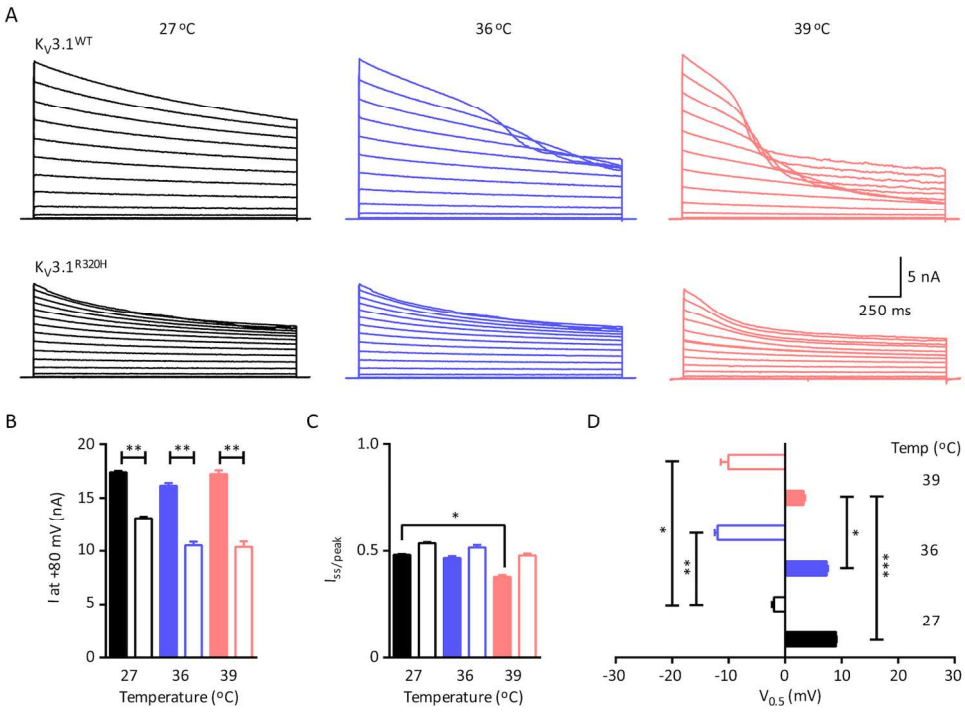

Effect of increased temperature on KV3.1WT and KV3.1WT+R320H mutant channels. (A) Representative current family traces, for KV3.1WT (top panel) and KV3.1WT+R320H (bottom panel) at 27 oC (black), 36 oC (blue) and 39 oC (pink). Scale bars apply to all traces. (B) Average peak current-voltage relationship curves for KV3.1WT () and KV3.1WT+R320H () at 27 oC (black), 36 oC (blue) and 39 oC (pink). KV3.1WT (n = 45), 36 oC (n = 25) and 39 oC (n = 20) and KV3.1WT+R320H channels 27 oC (n = 41), 36 oC (n = 19) and 39 oC (n = 14). Statistical significance marked as ** p<0. 01; *** p<0.001; **** p<0.0001.

Fig 5

170x139mm (300 x 300 DPI)

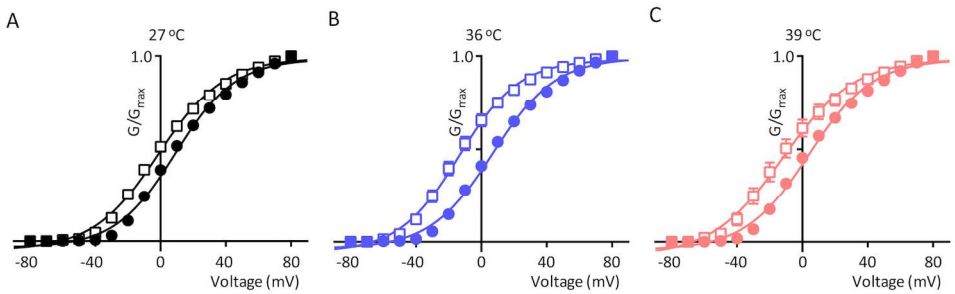

Temperature dependent effects on channel conductance. (A) Voltage-dependence of normalised peak conductance shown for KV3.1WT () and KV3.1WT+R320H () as a function of voltage at 27 oC (black), 36 oC (blue) and 39 oC (pink). Boltzmann curves were fit to pooled averages. (B) Comparison of the average voltage of half activation (V0.5) for KV3.1WT (solid bars) and KV3.1WT+R320H (open bars) at 27 oC (black), 36 oC (blue) and 39 oC (pink). KV3.1WT channels 27 oC (n = 45), 36 oC (n = 25) and 39 oC (n = 20) and KV3.1WT+R320H channels 27 oC (n = 41), 36 oC (n = 19) and 39 oC (n = 14). Statistical significance marked as * p<0.05; ** p<0.01; *** p<0.001.
Fig 6
170x49mm (300 x 300 DPI)

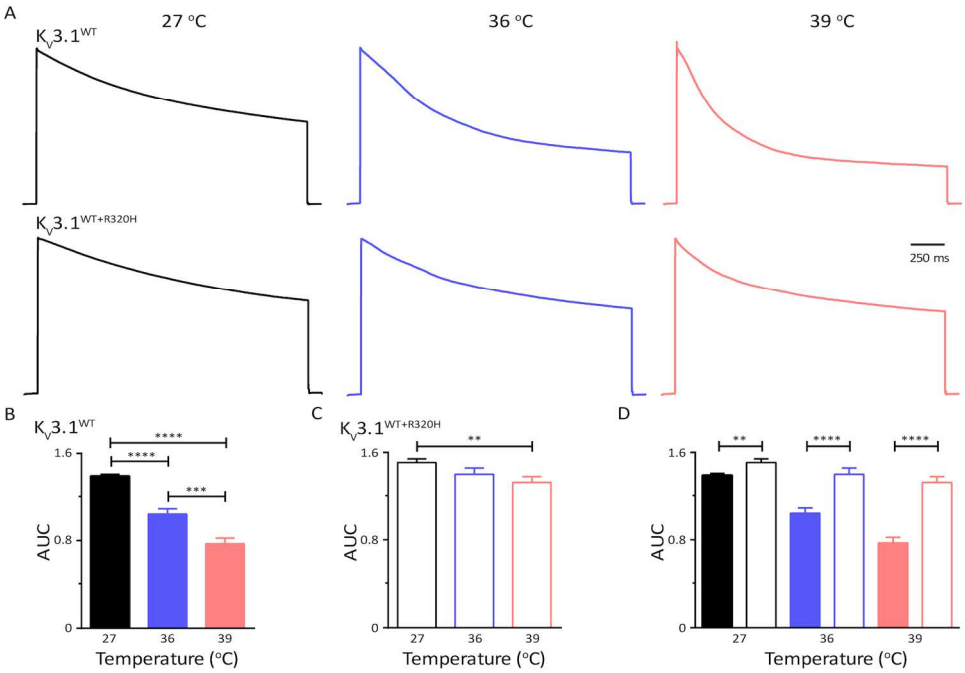

Temperature dependent effects on channel inactivation. (A) Mean of current traces recorded at +80 mV and normalised to the peak current for KV3.1WT (top panel) and KV3.1WT+R320H (bottom panel) at 27 oC (black), 36 oC (blue) and 39 oC (pink). Scale bar applies to all traces. (B) Inactivation for KV3.1WT was quantified as area under the curve (AUC) at 27 oC (solid black), 36 oC (solid blue) and 39 oC (solid pink). (C) Inactivation for KV3.1WT+R320H was quantified as AUC at 27 oC (open black), 36 oC (open blue) and 39 oC (open pink). (D) Comparison of AUC values for KV3.1WT (solid bars) and KV3.1WT+R320H (open bars) at 27 oC (black), 36 oC (blue) and 39 oC (pink). All AUC values were calculated from panel A. KV3.1WT channels 27 oC (n = 45), 36 oC (n = 25) and 39 oC (n = 20) and KV3.1WT+R320H channels 27 oC (n = 41), 36 oC (n = 19) and 39 oC (n = 14). Statistical significance marked as ** p<0.01; *** p<0.001; **** p<0.0001.

Fig 7

170x113mm (300 x 300 DPI)

Supplementary Table. MEAK progressive myoclonus epilepsy clinical characteristics and seizure types in 20 patients.

Patient identifier	Gender	Year born	Birth and early development	Seizures types (onset)	Cerebellar signs	Mild cognitive decline (onset)	Treatment	Positive response to fever	Outcome
Case 1 (PME8-1)*	Male	1973	Normal	Myoclonus (12y) GTCS (15y)	Ataxia Dysmetria Hypotonia Dysarthria	Yes (30y)	**Current: CZP, LTG, VPA, ZNS** Past: BRV, PB, PIR, PRM	Yes	Living 42 years Wheelchair at 27 Fully dependent
Case 2 (PME10-1)*	Male	1975	Normal	Myoclonus (6y) GTCS (10y)	Ataxia Dysmetria Hypotonia Dysarthria Brisk tendon reflexes	Possibly	**Current: CLB, CZP, PIR, VPA** Past: CBZ, PB	N/A	Living 40 years Wheelchair at 17 Fully dependent
Case 3 (PME17-1)*	Male	1973	Normal	GTCS (6y) Myoclonus (8y)	Ataxia** Dysmetria	No	**Current: BRV, CZP, PPL, VPA, ZNS,** Past: LEV, PB, PIR	No	Living 42 years Wheelchair at 16 Fully dependent
Case 4 (PME18-1)*	Female	1977	Normal	Myoclonus / "tremor" (7y) GTCS ("school age") Possible absence ("school age")	Ataxia Dysarthria Mild dysmetria	Yes ("school age")	**Current: VPA, TPM, LEV** Past: CBZ, CZP, ETX, PIR, STM	No	Living 38 years Wheelchair at 15 Fully dependent
Case 5 (PME29-1)*	Male	1989	Mild learning difficulties	Myoclonus / "tremor" (9y) GTCS (10y)	Ataxia	No	**Current: PER, VPA, ZNS** Past: CLB, CZP, ETX, KD, LEV, LTG, STM, TPM	No	Living 26 years Cautiously ambulant Remains independent (works part-time)
Case 6 (PME36-1)*	Female	1991	Normal	Myoclonus / "tremor" (7y) GTCS (10y)	Ataxia Dysarthria	No	**Current: AZA, DZP, TPM** Past: CZP, GBP, LEV, LTG, MAD, PIR, PRM, VGB, VPA, ZNS	Yes	Living 24 years Wheelchair at 14 Mostly dependent
Case 7 (PME37-1)*	Female	1994	Normal	Myoclonus (10y) GTCS (13y)	Ataxia Dysarthria	No	**Current: CZP, LEV, ZNS** Past: VPA	N/A	Living 21 years Wheelchair at 17 Fully dependent

Patient identifier	Gender	Year born	Birth and early development	Seizures types (onset)	Cerebellar signs	Mild cognitive decline (onset)	Treatment	Positive response to fever	Outcome
Case 8 (PME44-1)*	Female	1989	Normal	Myoclonus / "tremor" (12y) GTCS (14y)	Ataxia Dysarthria	Yes (15y)	**Current: CZP, LEV** Past: PPL, PRM, VPA	Yes	Living 26 years Walking aide at 14 Mostly dependent
Case 9 (PME63-1)*	Female	1988	Normal	Myoclonus (9y) GTCS (9y)	Ataxia Dysarthria Mild dysmetria	Possibly	**Current: CZP, VPA, ZNS** Past: LEV, PIR	N/A	Living 27 years Wheelchair at 13 Fully dependent
Case 10 (PME65-1)*	Female	1988	Normal	Myoclonus (9y) GTCS (10y)	Ataxia Dysarthria	Yes (10y)	**Current: LEV, VPA, ZNS** Past: CZP, LTG, PB	No	Living 27 years Wheelchair at 15 Fully dependent
Case 11^ (PME84-1)*	Female	1971	Normal	Myoclonus / "tremor" (10y) GTCS (16y)	Ataxia Dysarthria	Yes (10y)	**Current: AZA, CZP, VPA** Past: TPM	No	Living 44 years Comfortably ambulant Remains independent
Case 12^ (PME84-2)*	Female	1976	Mild developmental delay and learning difficulties	Myoclonus / "tremor" (13y) GTCS (13y)	Ataxia Dysmetria	Yes ("school age")	**Current: AZA, BAC, CZP, VPA**	No	Living 39 years Cautiously ambulant Remains independent
Case 13^ (PME84-3)*	Male	1994	Mild developmental delay, learning and behavioural difficulties	Myoclonus / "tremor" (11y) GTCS (12y)	Ataxia Dysarthria	Yes (15y)	**Current: AZA, BAC, CZP, TPM**	No	Living 21 years Cautiously ambulant Remains independent
Case 14^ (PME84-4)*	Female	1997	Mild developmental delay and learning difficulties	Febrile seizures (8m) GTCS (14y) Myoclonus / "tremor" (unknown)	Dysmetria Clumsy gait when running	No	**Current: TPM**	No	Living 18 years Comfortably ambulant Remains independent
Case 15 (Secondary 1)*	Male	1995	Normal	Febrile seizures (6m) Myoclonus (10y) GTCS (10y)	Ataxia Dysmetria Dysdiadochokinesia	Yes (12y)	**Current: LEV, VPA, ZNS** Past: CBZ, LGIT, LTG, PIR, RFM, TPM	N/A	Living 20 years Cautiously ambulant Remains independent
Case 16 (Secondary 2)*	Male	1963	Normal	GTCS (9y) Myoclonus (12y)	Ataxia Dysarthria	No	**Current: VPA**	Yes	Living 52 years Wheelchair in teens Fully dependent

Patient identifier	Gender	Year born	Birth and early development	Seizures types (onset)	Cerebellar signs	Mild cognitive decline (onset)	Treatment	Positive response to fever	Outcome
Case 17	Male	1997	Normal	Myoclonus / "tremor" (8y)	Ataxia Dysarthria Dysmetria	No	**Current: AZA, CZP, PIR, VPA**	Yes	Living 18 years Cautiously ambulant Remains independent
Case 18^^	Male	1998	Normal	GTCS (12y) Myoclonus (13y)	Ataxia	Yes (16y)	**Current: CZP, VPA** Past: LEV	No	Living 17 years Wheelchair at 17 Fully dependent
Case 19^^	Female	1975	Mild learning difficulties	Myoclonus / "tremor" (15y) GTCS (15y)	Ataxia Dysarthria Dysmetria Dysdiadochokinesia	Yes ("school age")	**Current: LEV, VPA** Past: CBZ, LTG, PB, VGB	No	Living at 40 years Cautiously ambulant Living independently
Case 20	Male	1952	Mild learning difficulties	Myoclonus / "tremor" (9y) GTCS (9y)	Ataxia Dysarthria Dysmetria Dysdiadochokinesia	Yes (14y)	**Current: CZP, DZP, PB, VPA, ZNS** Past: ETX, LEV	Yes	Deceased at 63 years Wheelchair at 18 Fully dependent

* reported in Muona et al 2015; **note early onset at 3 years with ataxia; ^Family 1; ^^Family 2; N/A - no recent periods of fevers

AZA = Acetazolamide; BAC = Baclofen; BRV = Brivaracetam; CBZ = Carbamazepine; CLB = Clobazam; CZP = Clonazepam; DZP = Diazepam; ETX = Ethosuximide; GBP = Gabapentin; KD = ketogenic diet; LEV = Levetiracetam; LGIT = low glycemic index treatment; LTG = Lamotrigine; MAD = modified atkins diet; PB = Phenobarbitone; PIR = Piracetam; PPL = Perampanel; PRM = Primidone; RFM = Rufinamide; STM = Sulthiame; TPM = Topiramate; VGB = Vigabatrin; VPA = Valproic Acid; ZNS = Zonisamide